The 3rd International Conference on Structural Health Monitoring of Intelligent Infrastructure
Vancouver, British Columbia, Canada
November 13-16, 2007

WAVELET DECOMPOSITION APPROACH FOR ARCHIVING AND QUERYING LARGE VOLUME OF STRUCTURAL HEALTH MONITORING DATA

Yusuke Mizuno
The University of Tokyo, Japan

Yozo Fujino
The University of Tokyo, Japan

Abstract

This paper presents a method, which can be implemented under limited resources such as wireless sensor network devices, for archiving and extracting significant features of vibration responses of civil structures. The method is applied to waves from structural vibration response, and consists of Fourie transform, Haar wavelet decomposition, thresholding, quantization, and differentiating metric. Before the differentiating metric, a target signal is compressed into the wavelet coefficients "signature". The results indicate that a single measurement point without time synchronization of other measurement points is effective for instant damage detection through the case study using the ASCE SHM benchmark program. It is also shown that the method can reduce the data to a small fraction of an original data volume, while retaining enough information to detect structural damage and its severity. The approach illustrated in this paper implies a promise of wavelet-based data compression and analysis for the increasing volume of Structural Health Monitoring (SHM) data.

INTRODUCTION

As a number of new wireless sensor network based approaches such as Lynch et al. (2004) and Nagayama et al. (2004) have been explored as well as conventional monitoring systems can store and exchange data less expensively, the available volume of sensing data for structural health monitoring (SHM) of civil structures is increasing explosively. This trend will continue due to the advent of affordable and high-speed wired and wireless networks, and enormous data storage space both online and offline environments. The availability of the huge amount of health monitoring data inspires damage detection methods, precise damage estimation, and other SHM-related projects as shown in Sohn et al. (2003).

A variety of damage detection methods have been developed and discussed. Mattson and Pandit (2006) proposed a method based on vector autoregressive (ARV) models to provide an accurate diagnosis of damage condition. Sohn et al. (2004) and Queck et al. (2001) developed wavelet-based damage detection methods. Development of a damage detection method is usually based on specific structures and environments including external forces.

The methods for damage detection shown above assume relatively rich environments in terms of data acquisition and computation. Time synchronization of data sources is usually one of the most critical issues, as Lei et al. (2005) described. Power efficiency is also one of the challenging topics in the field of wireless sensor network, as Lynch et al. (2004) presented. Although the limitations that preclude wireless data acquisition and transmission will become less in the log term as mentioned in the beginning, there still remains a trade-off between rich resources and power consumption. Data transmission is usually one of the critical issues on power consumption at this moment. This paper focuses on a data compression method for reducing data transmission with a capability of damage detection. In application, we assume a two-tier architecture which consists of wireless sensor nodes, and parent nodes designed to both store and process data from sensor nodes. Sensor nodes send only a small fraction of all data in order to reduce power consumption due to data transmission, and do not store the past records.

The objective of this paper is to develop a damage detection method that consists of a simple and fast computation algorithm which can be embedded on a platform with limited resources, that provides efficient and robust data compression, and with which a single sensor unit can detect the existence of damage and give an indication of the cumulative severity of damage in a structure.

WAVELET DECOMPOSITION FOR FEATURE EXTRACTION AND DAMAGE DETECTION

Signature Distillation

The method proposed in this paper is inspired by the image processing method that Jacobs et al. (1995) developed for fast image querying. The fundamental idea is quite simple: compressing both target and reference signals to "signatures", and comparing them. The signature distillation process is easily expanded to three or more dimensions and shrunk to one dimension.

The flow of the method starts with wavelet decomposition transferring acceleration or other response signals to wavelet coefficients. Then, thresholding eliminates small amplitude coefficients. Finally, quantization converts each coefficient to either -1, 0 or +1 in order to generate the signatures. The difference between the signatures of the target (probably damaged) and reference (usually undamaged) signals provides an index of the similarity of the two signals, from which we can detect the existence and the severity of damage.

Wavelet Decomposition

Wavelet transforms are powerful tools to capture the trend of target signals. They often produce similar outputs with time-frequency analysis methods such as short time Fourier transform and Gabor transform. They are also effective in reconstructing and signal representation and compression.

Haar wavelet decomposition uses two functions: the box function ϕ, also called the scaling function, and the mother wavelet ψ, which is the difference of two half-boxes. They are defined as

$$\phi(t) = \begin{cases} 1 & for\ \ 0 \le t < 1 \\ 0 & otherwise \end{cases} \quad , \quad \psi(t) = \begin{cases} 1 & for\ \ 0 \le t < 1/2 \\ -1 & for\ \ 1/2 \le t < 1 \\ 0 & otherwise \end{cases} \tag{1}$$

From the mother wavelet ψ, scaled and time-shifted functions ψ_{jk} are constructed as follows:

$$\psi_{jk}(t) = 2^{j/2}\psi\left(2^j t - k\right) \qquad j,k \in \mathbb{Z} \tag{2}$$

The subscripts j and k denote the time shift and the scale respectively. A shifted wavelet ψ_{0k} is non-zero in the interval $[k, k+1)$. A rescaled wavelet ψ_{j0} is scaled by a factor 2^{-j} in time and $2^{j/2}$ in amplitude. It is shown that the family $\left(\psi_{jk}\right)_{j,k\in\mathbb{Z}}$ is an orthonormal base of $L^2(\mathbb{R})$, which means that any real-valued function of time f such that $\int_{-\infty}^{\infty}\left|f^2(t)\right|dt$ is finite can be decomposed as

$$f(t) - \sum_{j,k} b_{jk}\psi_{jk}(t) \tag{3}$$

$$\text{with} \quad b_{jk} =< f, \psi_{jk} >= \int_{-\infty}^{\infty} f(t)2^{j/2}\psi\left(2^j t - k\right)dt \tag{4}$$

The coefficients b_{jk} are called wavelet coefficients. From the scaling function ϕ, functions ϕ_{jk} are also constructed, and scaling coefficients defined as $a_{jk} =< f, \phi_{jk} >$.

From Eq.(1), it follows that the ϕ_{jk} and ψ_{jk} satisfy the dilation equation (5), and the wavelet equation (6)

$$\phi_{j-1,k}(t) = \frac{1}{\sqrt{2}}[\phi_{j,2k}(t) + \phi_{j,2k+1}(t)] \tag{5}$$

$$\psi_{j-1,k}(t) = \frac{1}{\sqrt{2}}[\phi_{j,2k}(t) - \phi_{j,2k+1}(t)] \tag{6}$$

By multiplying by $f(t)$ and integrating, relations between the coefficients are obtained:

$$a_{j-1,k} = \frac{1}{\sqrt{2}}[a_{j,2k} + a_{j,2k+1}] \tag{7}$$

$$b_{j-1,k} = \frac{1}{\sqrt{2}}[a_{j,2k} - a_{j,2k+1}] \tag{7}$$

These show that the coefficients follow a recursive algorithm. Consider the signal of length $N = 2^m$ given by array $A = [a_0, a_1, \cdots, a_N]$. The subscripts of each element A are first renamed to $A = [a_{m0}, a_{m1}, \cdots, a_{mN}]$. By applying recursive algorithms shown in Eq. (7) and (8), the decomposition produces the Haar wavelet coefficients given by the array

$B = [a_{00}, b_{00}, b_{01}, \cdots, b_{m-1, 2^{m-1}-1}]$.

Haar wavelets offer a simple and fast computation metric which can be embedded in devices with small computation and storage capabilities such as web-enabled phones, PDAs and embedded PCs. The significant results obtained with the Haar wavelet decomposition are described in the case study section.

Thresholding, Quantization and Differentiating Metric

Thresholding eliminates small amplitude coefficients derived by the decomposition shown above, and the largest coefficients remain. Quantization makes positive coefficients being large enough for thresholding +1, negative coefficients -1. The rest of the coefficients, which are eliminated through thresholding, hold the value 0. The processed (by both thresholding and quantization) coefficients are given by array to simplify the notation for the differentiating metric shown below. The number of coefficients remaining in the stage of thresholding is referred as "threshold number" in the rest of the paper. There is a trade off between the data volume, when stored and transmitted, and the threshold number.

We introduce a differentiating metric to define a distance between signatures, based on that in Jacobs et al. (1995). The distance between the signatures of a reference signal B^r and a target signal B^t according to this metric is defined as

$$\left\| B^t, B^r \right\| = \sum_j w_j \left| \tilde{b}_j^t - \tilde{b}_j^r \right| \qquad (8)$$

where w_j is a weight assigned to the j th element of the signature.

The weighted sum of the difference between the signature coefficients expresses the distance of two signals. The distance between two signatures will therefore be referred to as "difference index" in the rest of the paper. The smaller the difference index is, the more similar the target signal is to the reference one. Because each non-zero coefficient of the signature is equal to either -1 or 1, the difference index between two signatures is between 0 and two times the threshold number, when all the weights are set to 1.

The weights w_j may be obtained by statistical methods such as the one proposed by Jacobs et al. (1995), which used a statistical approach to find optimal weights for painted and scanned images. However, in this paper all the weights are set to 1 for the case study described below.

CASE STUDY – THE ASCE BENCHMARK PROBLEM

The ASCE Benchmark Problem, whose details are described by Johnson et al. (2004), is used as a test case to show the performance of the damage detection method proposed in this paper. The benchmark structure is a 4-storey, 2-bay by 2-bay steel frame structure as shown in Fig. 1. MATLAB codes to generate the benchmark data are available on the web site hosted by the ASCE Structural Health Monitoring Committee.

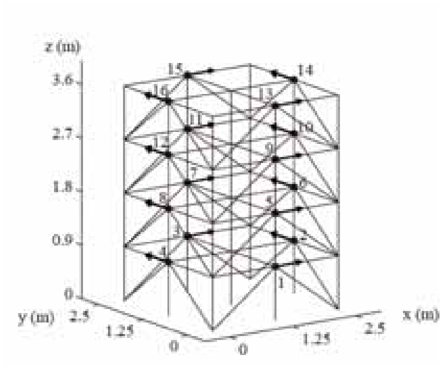

Figure 1. Benchmark structure, and sensor locations and directions

Two finite element models, a 12 degree of freedom (DOF) shear-building model and a 120-DOF model, were developed to generate the simulated response data. Six cases were defined, which had different properties: degrees of freedom; mass distribution; excitation. The six predefined damage patterns are: (i) no stiffness in the braces of the first story; (ii) no stiffness in the braces of the first and third stories; (iii) no stiffness in one brace in the first story; (iv) no stiffness in one brace in the first story and one brace in the third story; (v) the same as damage pattern (iv) but with a floor beam at the first level partially unscrewed; and (vi) two thirds stiffness in one brace in the first story.

Time Domain Analysis

Only data from the 120-DOF model is used in this paper. Case 5 has an asymmetric mass distribution on the roof and a shaker placed diagonally on the roof. Seven output responses (for the undamaged structure and the six damage patterns) with default parameters except for the duration, modified to 41 seconds, were generated. As mentioned in Johnson et al. (2004), in the benchmark the external forces are modeled by Gaussian white noise passed through a sixth order low-pass Butterworth filter with a 100 Hz cut off frequency, and the Fourier transform of a sample response showed that the signal has no significant power in frequencies beyond 100Hz. The response acceleration data is thus down sampled to 200Hz.

Table 1. Normalized difference indices in time domain (sensor 13)

		Damage pattern						
		0	1	2	3	4	5	6
Damage pattern	0	0.00	0.95	0.95	0.19	0.87	0.87	0.07
	1		0.00	0.76	0.96	0.95	0.95	0.95
	2			0.00	0.95	0.93	0.93	0.95
	3				0.00	0.83	0.83	0.16
	4					0.00	0.01	0.85
	5						0.00	0.84
	6							0.00

Table 1 shows a result for the case where the threshold number is set to 256. It also describes detailed comparison between damage patterns. Damage patterns 1, 2, 4 and 5 are clearly distinguished from the undamaged pattern by the difference indices.
When different seed numbers are used for the input force generation, the proposed approach cannot detect damage. The difference index is very sensitive to changes in time histories such as those due to external forces generated by different random seed numbers.

Frequency Domain Analysis

It is straightforward to convert target signals into Fourier coefficients in order to capture the structural behavior. In the following, the performance of frequency domain analysis using Haar wavelet decomposition is investigated.

The response acceleration data is down sampled to 200Hz in the same way as for time domain analysis and the fast Fourier transform algorithm (FFT) is applied to the first 8,192 points to obtain 4,096 Fourier amplitudes. Fig. 2 shows the effect of the threshold number on the results for acceleration responses at sensor 14 in frequency domain. Each plotted point is a mean value of normalized difference indices of each damage pattern. The indices of the target signals are obtained by simulations with seed numbers varying from 1 to 256 except 123, and the reference signal is generated by an undamaged simulation using the default seed number 123. For both the smallest and largest threshold numbers, no damage pattern can be distinguished from the undamaged case.

Figure 3 also shows the effect of the data length in time domain on the results for acceleration responses at sensor 14 in frequency domain, where the threshold number holds the same number 128. It is shown that more than 4,096 raw data is enough to detect damage.

Figures 4 and 5 illustrate a typical difference index distribution for x-axis and y-axis sensors respectively. Each distribution is displayed in the form of a boxplot, which consists of the largest non-outlier observation, upper quartile (UQ), median, lower quartile (LQ), and smallest non-outlier observation. Outliers are plotted as circles. Damage patterns 1 and 2 are easily separated from the undamaged case and damage patterns 4 and 5 are also detectable but with smaller gaps in both figures. Damage patterns 3 and 6 are hardly distinguished from the undamaged case in Fig. 4. Damage pattern 3 is also distinct from the undamaged case in Fig.5. Still a large overlap exists between damage pattern 6 and the undamaged case, which shows the limitation of the proposed method: very slight damage such as only one third stiffness reduction in one brace is not detected.

It appears that the difference index is proportional to the number of damaged elements. When damage patterns are sorted by decreasing the number of damaged elements, the list “2, 1, 5, 4, 3, 6” is obtained. The same list is obtained when damage patterns are sorted by decreasing difference index, except for damage patterns 4 and 5 which have almost the same difference index, and differ only in the fact that for damage pattern 5, only one floor beam is partially unscrewed.

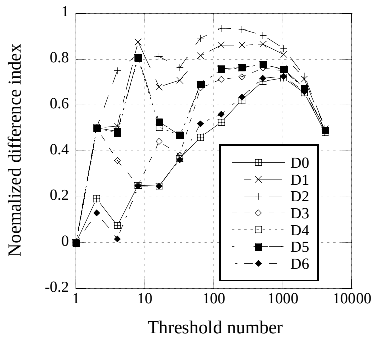

Figure 2. Effect of the threshold number in frequency domain

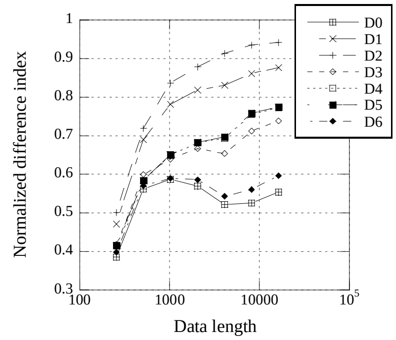

Figure 3. Effect of the data length in frequency domain

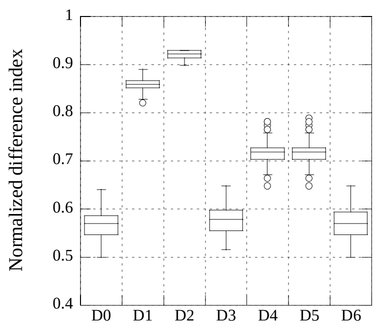

Figure 4. Frequency domain analysis (sensor 13, threshold number 128)

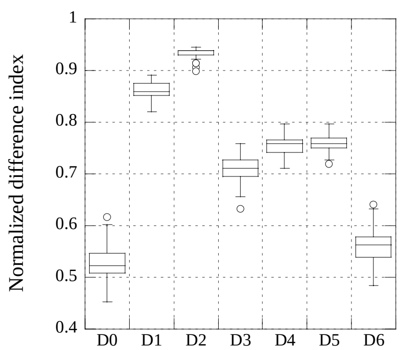

Figure 5. Frequency domain analysis (sensor 14, threshold number 128)

The analysis developed in frequency domain requires more computation load before distilling the signature. But when this method is applied, it drastically reduces the volume of data transmission. Only 128 non-zero coefficients among 8,192 raw data points are used in this analysis, which means that using less than 5% of the original data volume is enough to detect all damage cases except damage pattern 6.

DATA ARCHIVING FOR SENSING DATA

The feature extraction method described in this paper can be used as compressing sensing data in order to reduce the volume when transmitted from a sensor node to a data storage server or a data processing node. As shown in the case study the proposed method shows an adequate performance of damage assessment. In the case where raw sensing data is required for further investigation, the signature distilled from raw data functions as an index when querying among the large volume of data records.

CONCLUSIONS

This paper presents a damage detection method using wavelet decomposition. Reference and target signals are processed by means of Haar wavelet decomposition, thresholding, and finally quantization, to obtain a compressed version of each signal, called "signature". A different matrix is finally used to compare the signatures of reference and target signals, and thus identify damage. Through the ASCE Benchmark Problem, the method revealed a potential to skim through large amounts of sensing data. It could also significantly compress raw measured data.

The algorithm proposed in this paper is simple and fast enough to detect damage and is a promising distributed sensor system for SHM. The case study reveals that only 128 signature coefficients computed from 8,192 raw data points are enough to detect five of the six predefined damage cases. This corresponds to only less than 5% of the original data. Also, the proposed method does not require time-synchronization between sensor nodes since only frequency amplitudes are used to compute the signatures.

REFERENCES

1. Lynch, J. P., Sundararajan, A., Law, K. H., Kiremidjian, A. S., and Carryer, E., 'Embedding damage detection algorithms in a wireless sensing unit for operational power efficiency', Smart Materials and Structures, 13 (2004) 800-810.
2. Nagayama, T., Ruiz-Sandoval, M., Spencer Jr., B.F., Mechitov, K.A., and Agha, G.., 'Wireless Strain Sensor Development for Civil Infrastructure', Proceedings of First International Workshop on Networked Sensing Systems, Tokyo, Japan, (2004) 97-100.
3. Sohn, H., Farrar, C. R., Hemez, F. M., Shunk, D. D., Stinemates, D. W., and Nadler, B. R., A Review of Structural Health Monitoring Literature: 1996-2001. Los Alamos National Laboratory Report, LA-13976-MS, (2003).
4. Mattson, S. G., and Pandit, S. M., 'Statistical moments of autoregressive model residuals for damage localization', Mechanical Systems and Signal Processing, 20: (2006) 627-645.
5. Sohn, H., Park, G., Wait, J.R., Limback, N. P, and Farrar, C. R., 'Wavelet-based active sensing for de-lamination detection in composite structures', Smart Materials and Structures, 13: (2004) 153-160.
6. Queck, S. T., Wang, Q., Zhang, L., and Ong, K.H., 'Practical issues in the detection of damage in beams using wavelets', Smart Materials and Structures, 10: (2001) 1009-1017.
7. Lei, Y., Kiremidjian, A. S., Nair, K. K., Lynch, J. P., and Law, K. H.., 'Algorithms for time synchronization of wireless structural monitoring sensors', Earthquake Engineering and Structural Dynamics, 34: (2005) 555-573.
8. Jacobs, C., Finkelstein, A., and Salesin, D., 'Fast Multiresolution Image Querying', SIGGRAPH 95 Proceedings, Annual Conference Series, ACM SIGGRAPH, (1995) 277-286.
9. Johnson, E. A., Lam, H. F., Katafygiotis, L. S., and Beck, J. L., 'Phase I IASC-ASCE Structural Health Monitoring Benchmark Problem Using Simulated Data', Journal of Engineering Mechanics, ASCE, 130(1): (2004) 3-15.